ANTIOXIDANTS & REDOX SIGNALING
Volume 17, Number 8, 2012

DOI: 10.1089/ars.2011.4417

ORIGINAL RESEARCH COMMUNICATION

Fanconi Anemia Links Reactive Oxygen Species to Insulin Resistance and Obesity

Jie Li,[1] Jared Sipple,[1] Suzette Maynard,[1] Parinda A. Mehta,[2,3] Susan R. Rose,[3,4] Stella M. Davies,[2,3] and Qishen Pang[1,3]

Abstract

Aims: Insulin resistance is a hallmark of obesity and type 2 diabetes. Reactive oxygen species (ROS) have been proposed to play a causal role in insulin resistance. However, evidence linking ROS to insulin resistance in disease settings has been scant. Since both oxidative stress and diabetes have been observed in patients with the Fanconi anemia (FA), we sought to investigate the link between ROS and insulin resistance in this unique disease model. ***Results:*** Mice deficient for the Fanconi anemia complementation group A *(Fanca)* or Fanconi anemia complementation group C *(Fancc)* gene seem to be diabetes-prone, as manifested by significant hyperglycemia and hyperinsulinemia, and rapid weight gain when fed with a high-fat diet. These phenotypic features of insulin resistance are characterized by two critical events in insulin signaling: a reduction in tyrosine phosphorylation of the insulin receptor (IR) and an increase in inhibitory serine phosphorylation of the IR substrate-1 in the liver, muscle, and fat tissues from the insulin-challenged FA mice. High levels of ROS, spontaneously accumulated or generated by tumor necrosis factor alpha in these insulin-sensitive tissues of FA mice, were shown to underlie the FA insulin resistance. Treatment of FA mice with the natural anti-oxidant Quercetin restores IR signaling and ameliorates the diabetes- and obesity-prone phenotypes. Finally, pairwise screen identifies protein-tyrosine phosphatase (PTP)-α and stress kinase double-stranded RNA-dependent protein kinase (PKR) that mediate the ROS effect on FA insulin resistance. ***Innovation:*** These findings establish a pathogenic and mechanistic link between ROS and insulin resistance in a unique human disease setting. ***Conclusion:*** ROS accumulation contributes to the insulin resistance in FA deficiency by targeting both PTP-α and PKR. *Antioxid. Redox Signal.* 17, 1083–1098.

Introduction

Fanconi anemia (FA) is a genetic disorder that is associated with bone marrow failure, developmental defects, and an extremely high disposition to leukemia and other cancers(4, 20). Fifteen complementation groups encoded by the respective FANC genes (A, B, C, D1, D2, E, F, G, I, J, L, M, N, O, and P) have been identified thus far (4, 20, 27). Among them, mutations in the Fanconi anemia complementation group A *(FANCA)* and Fanconi anemia complementation group C *(FANCC)* genes have been identified in more than 70% of FA patients worldwide (4, 20, 27). One of the clinical hallmarks of FA is the metabolic disorder, which is manifested by diabetes and other abnormalities of glucose metabolism (10, 11, 41). A recent clinical investigation performed at our Medical Center shows that near half of the FA patients enrolled in the study had abnormalities in glucose metabolism (10). In addition, studies from several other Institutes

Innovation

The article presents biochemical and genetic evidence that links reactive oxygen species (ROS) to insulin resistance and obesity. Clinical data show that diabetes and other abnormalities of glucose metabolism are common among children and adolescents with the Fanconi anemia, but the underlying molecular etiology of the diabetes is not known. This study employs both cell-based and genetic models that establish a pathogenic and mechanistic link between ROS and insulin resistance in a unique human disease setting and, thus, highlights the fact that studying rare disorders can elucidate important new clinical and biological principles. In addition, our pairwise screen has identified factors that mediate the ROS effect on Fanconi insulin resistance, thus giving us a hope for applying these findings to clinical interventions.

Divisions of [1]Experimental Hematology and Cancer Biology, [2]Bone Marrow Transplant and Immune Deficiency, Cincinnati Children's Hospital Medical Center, Cincinnati, Ohio.
[3]Department of Pediatrics, University of Cincinnati College of Medicine, Cincinnati, Ohio.
[4]Division of Endocrinology, Cincinnati Children's Hospital Medical Center, Cincinnati, Ohio.

involving more FA patients found that abnormalities of glucose homeostasis were frequent (up to 81% of FA patients) and included hyperglycemia (impaired glucose tolerance or diabetes mellitus) and hyperinsulinemia (10, 11, 41). Notably, the FA female heterozygote is about six times more likely to develop diabetes than the general population (28, 41).

Studies conducted on FA patients and knockout mice indicate that reactive oxygen species (ROS) levels are increased in both models (25, 34). Pathological ROS can cause oxidative stress, which has been considered a critical factor in the pathogenesis of FA (8, 25, 33, 34). Significantly, recent studies have shown that the FA proteins play important roles in oxidative stress response (OSR) (26, 36, 37). One of the earliest events in OSR is tyrosine phosphorylation activated by protein tyrosine kinases (PTKs) (30, 47). Insulin receptor (IR), one of the PTKs, is phosphorylated by insulin binding and initiates the IR signaling pathway, which plays critical roles during glucose and lipid metabolism (22, 42, 49). The IR is activated through phosphorylation at multiple tyrosine residues of the beta-subunit, which then phosphorylates and recruits different substrate adaptors, including members of the insulin receptor substrate (IRS) family. Phosphorylated IRS-1 at Tyr302 can display binding sites for several signaling partners. Among them, PI3K has a major role in insulin function, mainly *via* the activation of the AKT/PKB and the PKCzeta cascades (6, 12, 17, 43). The IR signaling pathway can be activated or inhibited by ROS. Exposure to oxidants such as hydrogen peroxide (H_2O_2) can mimic the insulin effect and trigger the activation of IR by inducing the phosphorylation of the receptor at tyrosine residues 1158/1162/1163 ($IR^{Tyr1158/1162/1163}$) in multiple cell types, including rat adipocytes, hepatocytes, and human B- and T- lymphocytes (14, 44, 45). On the other hand, high levels of ROS increase the activity of the c-Jun NH2-terminal kinase (JNK) or double-stranded RNA-dependent protein kinase (PKR) (6, 29).

Since both oxidative stress and diabetes have been observed in patients with the FA, we sought to investigate the link between ROS and insulin resistance in this unique disease model characterized by abnormal ROS accumulation and dysfunctional OSR (25, 34, 38). The results indicate that FA mice show phenotypic features of insulin resistance, which are associated with elevated levels of ROS production in insulin-sensitive tissues of the mice. Treatment of the FA mice with the natural anti-oxidant Quercetin ameliorates the diabetes-prone phenotypes by restoring insulin signaling.

Results

Receptor tyrosine kinases array identifies defective IR signaling in FA

To identify tyrosine kinases involved in the OSR in FA cells, we used human phosphor-receptor tyrosine kinase (RTK) arrays to screen 78 different RTKs for differentially activated kinases in response to the oxidative stress induced by H_2O_2 treatment in human lymphoblastic cell lines (LCLs) derived from a normal donor (HSC93) or an FA patient assigned to the complementation group C (FA-C; HSC536). We found that tyrosine phosphorylation of IR was selectively and significantly decreased in FA-C cells compared with normal cells (Fig. 1), suggesting impaired OSR-induced insulin signaling in FA cells. To demonstrate that the impaired insulin signaling also occurred in other FA complementation groups, we stimulated another pair of LCLs derived from a normal donor (JY) or an FA-A patient (HSC72) with or without insulin, and conducted a similar tyrosine kinase array. We were able to show that IR phosphorylation was also decreased in FA-A cells (Supplementary Fig. S1; Supplementary Data are available online at www.liebertonline.com/ars). To confirm the array results, we analyzed the tyrosine phosphorylation of IR in normal, FA-A, and FA-C cells. Again, we observed decreased IR tyrosine phosphorylation in FA cells, suggesting that FA deficiency impairs insulin signaling (Fig. 1E).

FA mice show diabetes-prone

Insulin signaling is critical for the regulation of glucose levels and the avoidance of diabetes mellitus; whereas defective insulin signaling may cause insulin resistance, leading to multiple diseases, including type 2 diabetes (T2D) and obesity (23, 46). Since cells from FA patients show impaired insulin signaling, we hypothesized that the diabetes-prone phenotypes observed in FA patients are due to insulin resistance. We, thus, sought to address the consequence of FA deficiency on insulin-regulated glucose metabolism using two FA knockout mouse models: $Fanca^{-/-}$ and $Fancc^{-/-}$. We observed higher fasting blood glucose, albeit not statistically significant, in both $Fanca^{-/-}$ and $Fancc^{-/-}$ mice compared with wild-type (WT) littermates (Fig. 2A). We also measured whole-body sensitivity to glucose or insulin in response to glucose/insulin challenge using the standard intraperitoneal (IP) glucose tolerance test (GTT) or insulin tolerance test (ITT). Glucose challenge induced a significant increase in whole-blood glucose in $Fanca^{-/-}$ or $Fancc^{-/-}$ mice compared with WT littermates (Fig. 2B). Similarly, persistent higher blood glucose levels were observed in $Fanca^{-/-}$ or $Fancc^{-/-}$ mice than in WT mice 30 min after an insulin injection (Fig. 2C). We also measured the serum levels of insulin in glucose-injected animals. Despite basal insulin levels being comparable between WT and FA mice, acute insulin release as measured at 5 min in response to glucose was increased by approximately twofold in both $Fanca^{-/-}$ and $Fancc^{-/-}$ mice when compared with their WT littermates (Fig. 2D). In addition, the fasting plasma insulin levels in $Fanca^{-/-}$ and $Fancc^{-/-}$ mice were nearly twice higher than those of WT mice (Fig. 2E). These results suggest the presence of insulin resistance in FA mice.

These results suggest that both $Fanca^{-/-}$ and $Fancc^{-/-}$ mice suffer from glucose intolerance and insulin resistance.

FA mice show obesity-prone

Since impaired insulin signaling is a key contributor to the pathogenesis of obesity (18), we next examined whether FA mice were susceptible to high-fat diet (HFD)-induced obesity. Both $Fanca^{-/-}$ and $Fancc^{-/-}$ mice were smaller than WT mice either at the embryonic stage (Fig. 3A) or at birth (Fig. 3B). Although there was no significant difference in food and water intake between genotypes (Supplementary Fig. S2), the size of the FA mice remained smaller after birth compared with their WT littermates with the normal chow (Fig. 3C, Supplementary Fig. S3). Remarkably, FA mice gained weight much faster than control animals after fed with HFD (Fig. 3D, E). Further, HFD had a profound effect on glucose/insulin metabolism, including significantly higher fasting blood glucose level (Fig. 3F) and reduced insulin tolerance (Fig. 3G), in FA mice compared with WT controls.

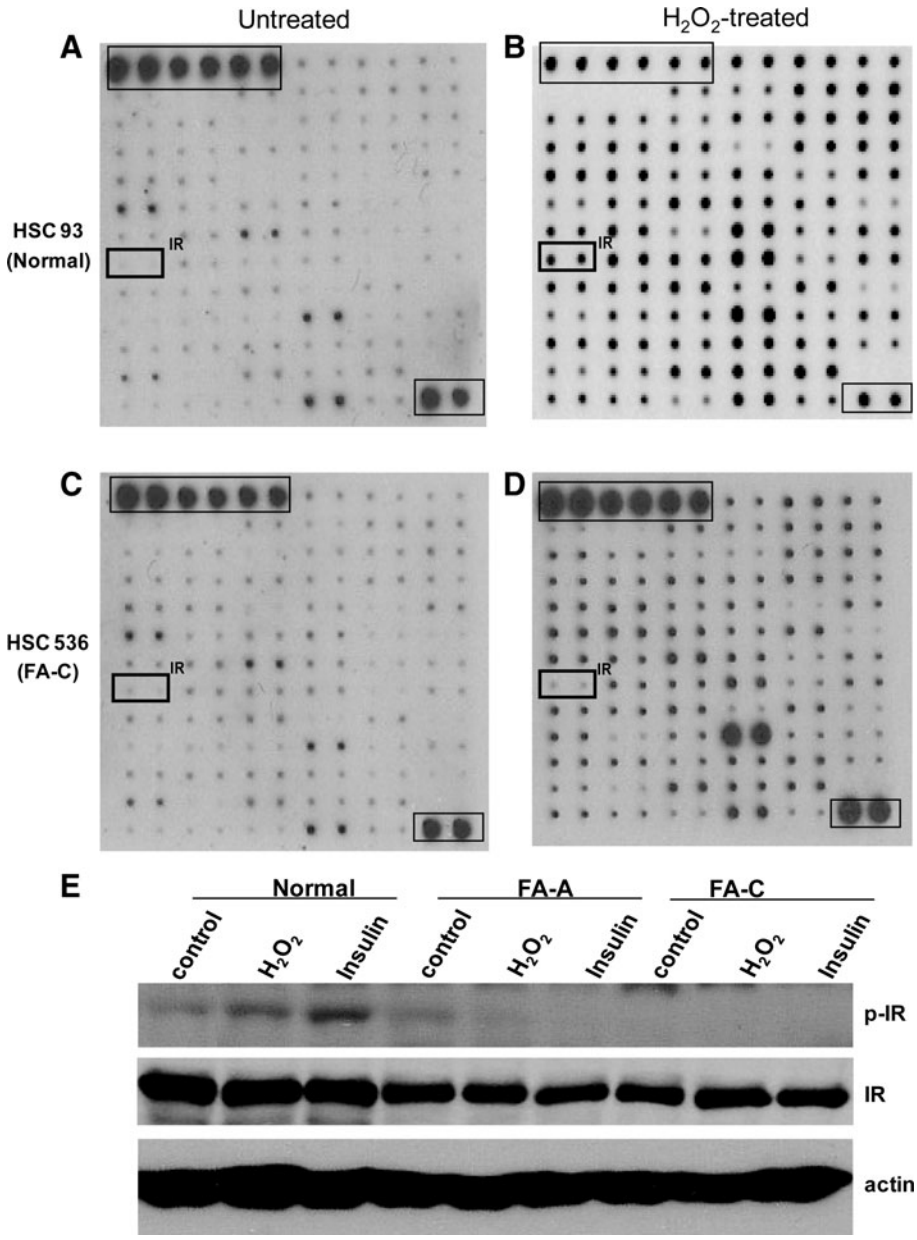

FIG. 1. RTK array identifies defective IR signaling in FA cells. **(A–D)** Human normal lymphoblastic cell line HSC93 **(A, B)** and FA-C patient-derived lymphoblastic cell line HSC536 **(C, D)** were treated with **(A, C)** or without **(B, D)** H_2O_2 (0.5 m*M*) for 15 min, and WCEs were subject to RTK array analysis. Phosphorylation status was determined by subsequent incubation with biotin-conjugated anti-phosphotyrosine antibody and streptavidin-linked horseradish peroxidase. Each RTK is spotted in duplicate, and the positive control includes six dots of the first layer and two dots of the last layer. **(E)** The indicated cells were treated with or without H_2O_2 (0.5 m*M*) or insulin (10 μg/ml) for 15 min. WCEs were separated by SDS-PAGE and probed with antibodies against phospho-IR and IR, and actin as loading control. FA, Fanconi anemia; H_2O_2, hydrogen peroxide; IR, insulin receptor; RTK, receptor tyrosine kinase; SDS-PAGE, sodium dodecyl sulfate polyacrylamide gel electrophoresis; WCEs, whole-cell extracts.

Biochemical analysis of insulin signaling in FA deficiency

To elucidate the molecular mechanism by which FA deficiency leads to insulin resistance and diabetes-prone, we examined insulin signaling in three insulin-responsive tissues, liver, fat, and skeletal muscle from *Fanca*$^{-/-}$ or *Fancc*$^{-/-}$ mice and their WT littermates. As shown in Figure 4A and B, the expression level of IR and AKT was comparable between the genotypes. However, insulin-stimulated phosphorylation of IR at tyrosine residues 1158/1162/1163 ($IR^{Tyr1158/1162/1163}$) was attenuated in all three tissues of both *Fanca*$^{-/-}$ and *Fancc*$^{-/-}$ mice compared with the WT controls (Fig. 4A, B). Consistent with this, AKT phosphorylation was also decreased in the FA mice (Fig. 4A, B). To verify the insulin-dependent signaling in a more defined *in vitro* system, we isolated beta cells from FA and WT mice, subjected the cells to insulin challenge, and examined activation of the insulin pathway by probing the phosphorylation of IR and AKT. As with the *in vivo* results just described, insulin-stimulated IR and AKT was reduced in FA beta cells compared with WT cells (Supplementary Fig. S4).

We next performed rescue experiments to confirm the role of FA proteins in insulin signaling. Due to the difficulties involved in viral transduction using primary insulin sensitive cells from mice, we used gene-corrected LCLs derived from an FA-A patient (HSC72) or an FA-C patient (HSC536) that genetically corrected with or without the human *FANCA* or *FANCC* gene, respectively. Consistent with the results in FA mice, we observed a marked reduction in the level of $IR^{Tyr1158/1162/1163}$, as well as tyrosine phosphorylation of the IRS-1, which activates insulin signaling (14), in insulin-induced FA LCLs compared with normal (JY) cells (Supplementary Fig. S5). As expected, insulin-stimulated phosphorylation of AKT was also markedly decreased in FA LCLs relative to normal controls (Fig. 4C). Correction of the

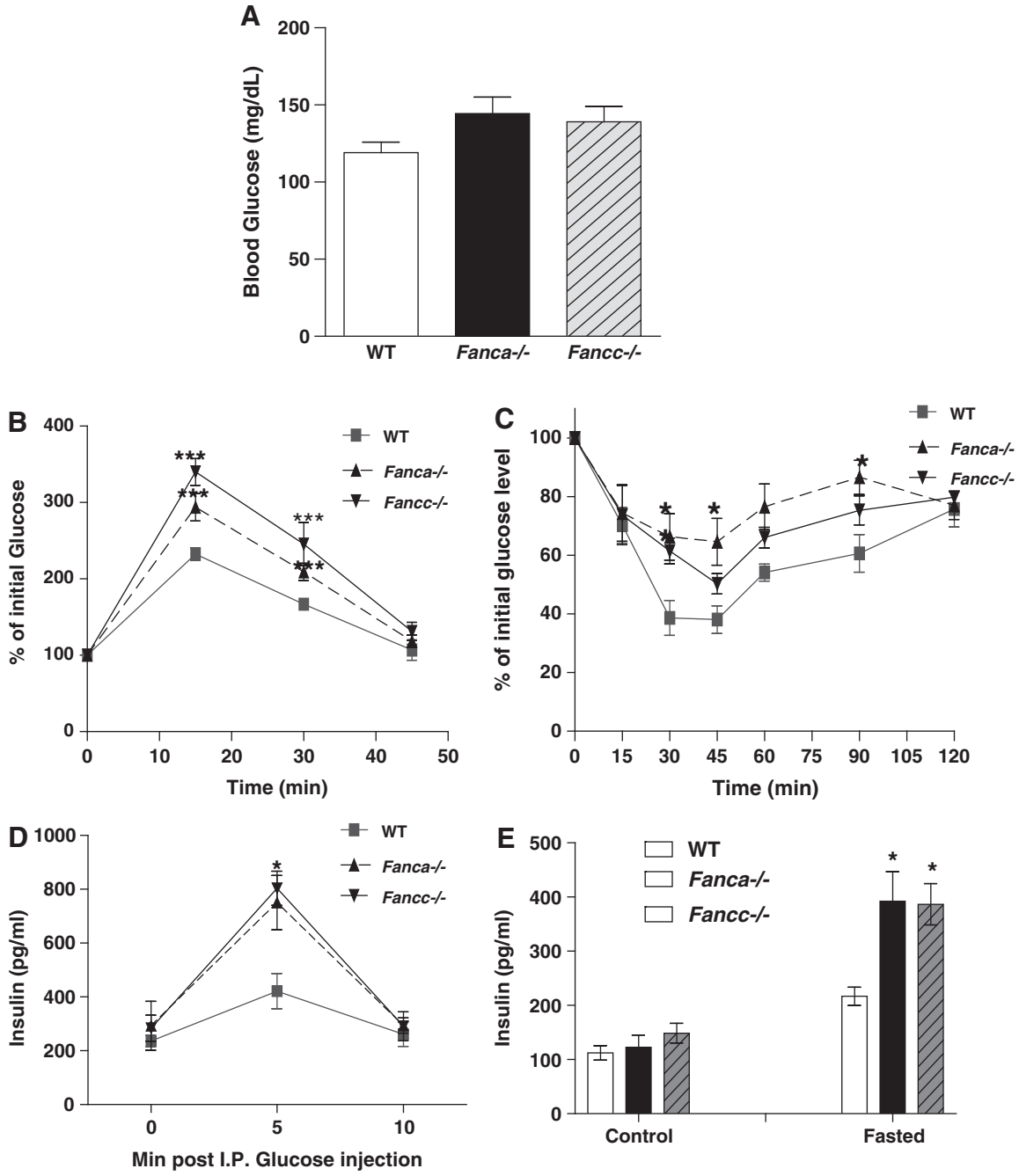

FIG. 2. FA mice seem to be diabetes mellitus prone. (A) Whole-blood glucose was measured in mice fasted overnight by using tail blood ($n = 6$–8 per genotype). **(B, C)** After having been fasted, mice (4–5 months old) were given an injection (IP) of either glucose (1 g/Kg of body weight) **(B)** or insulin (1.0 U/Kg of body weight) **(C)**, and whole-blood glucose was examined at the indicated time points by using the Glucometer. The results are shown as the percentage of the initial glucose levels. *$p < 0.05$, ***and $p < 0.001$ for *Fanca*$^{-/-}$ or *Fancc*$^{-/-}$ mice *versus* wt mice. **(D)** Increased acute-phase insulin release in FA mice. Mice were IP injected with glucose (1 g/kg body weight), and whole blood was collected from tail vein samples at the indicated times for insulin measurements. **(E)** Mice were fasted overnight, and whole blood was collected from tail vein samples at the indicated times for insulin measurements. Values are means ± SD ($n = 4$–6). *$p < 0.05$ *versus* WT. FANCA, Fanconi anemia complementation group A; FANCC, Fanconi anemia complementation group C; IP, intraperitoneal; WT, wild-type.

FA-A or FA-C cells with the human *FANCA* or *FANCC* gene, respectively, restored insulin responsiveness to the level comparable to normal cells (Fig. 4C). Conversely, knockdown of FANCA or FANCC in two insulin-sensitive cell lines, the human hepatocellular liver carcinoma cell HepG2 or mouse embryonic fibroblast-adipose like cell 3T3-L1, significantly reduced insulin-induced phosphorylation of both IR and AKT (Fig. 4D, Supplementary Fig. S6). Together, these rescue and knockdown experiments establish a role of the FA proteins in insulin signaling.

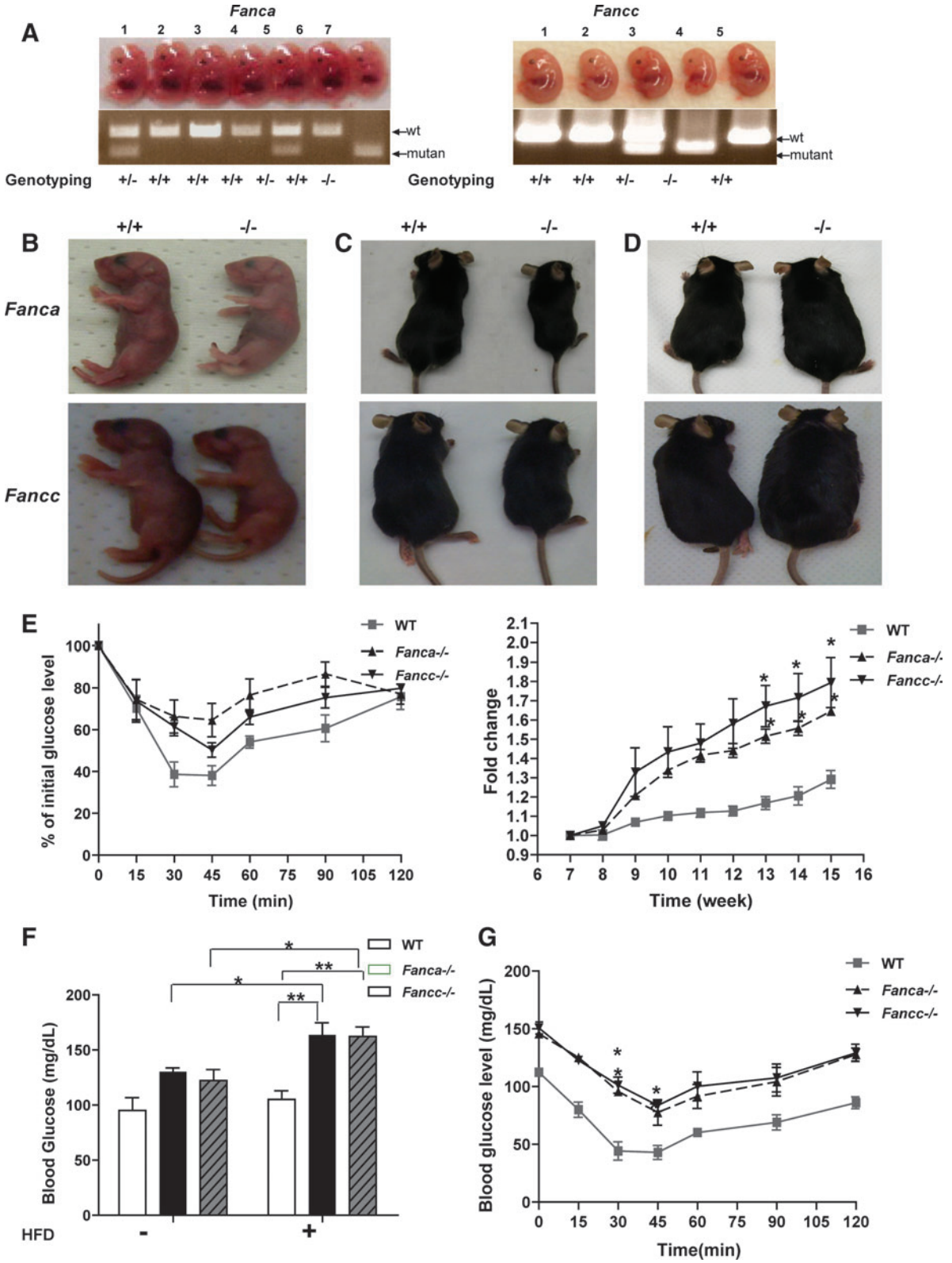

FIG. 3. FA mice show a high risk for diabetes induced by a high fat diet. **(A)** Images of embryos of the indicated genotypes at E12.5. Genotypes of the embryos were determined by PCR. **(B–D)** Size comparison between wt (+/+) and FA (−/−) mice at day one **(B)** or day 30 **(C)** after birth, or 4 months after being fed with HFD **(D)**. **(E)** wt or FA mice were fed with HFD starting at 7 weeks old, and the weight was examined at the indicated time points. The results are shown as the original readout (*left*) and fold increase from the starting weight (*right*). $*p<0.05$ for $Fanca^{-/-}$ or $Fancc^{-/-}$ mice *versus* wt mice. **(F)** Mice (8–9 weeks old, $n=6$–8 per genotype) were fed with HFD for 2 months, fasted overnight, and whole-blood glucose was measured using tail blood. $*p<0.05$; $**p<0.01$ for a comparison between groups of mice fed with HFD for 9 weeks versus before the feeding. **(G)** HFD-fed mice described in **(F)** were fasted overnight and given an injection (i.p) of insulin (1.0 U/Kg), and whole-blood glucose was examined at the indicated time points by using the glucometer. The results are shown as the original readout. $*p<0.05$ for $Fanca^{-/-}$ or $Fancc^{-/-}$ mice *versus* wt mice. HFD, high-fat diet. (To see this illustration in color the reader is referred to the web version of this article at www.liebertpub.com/ars).

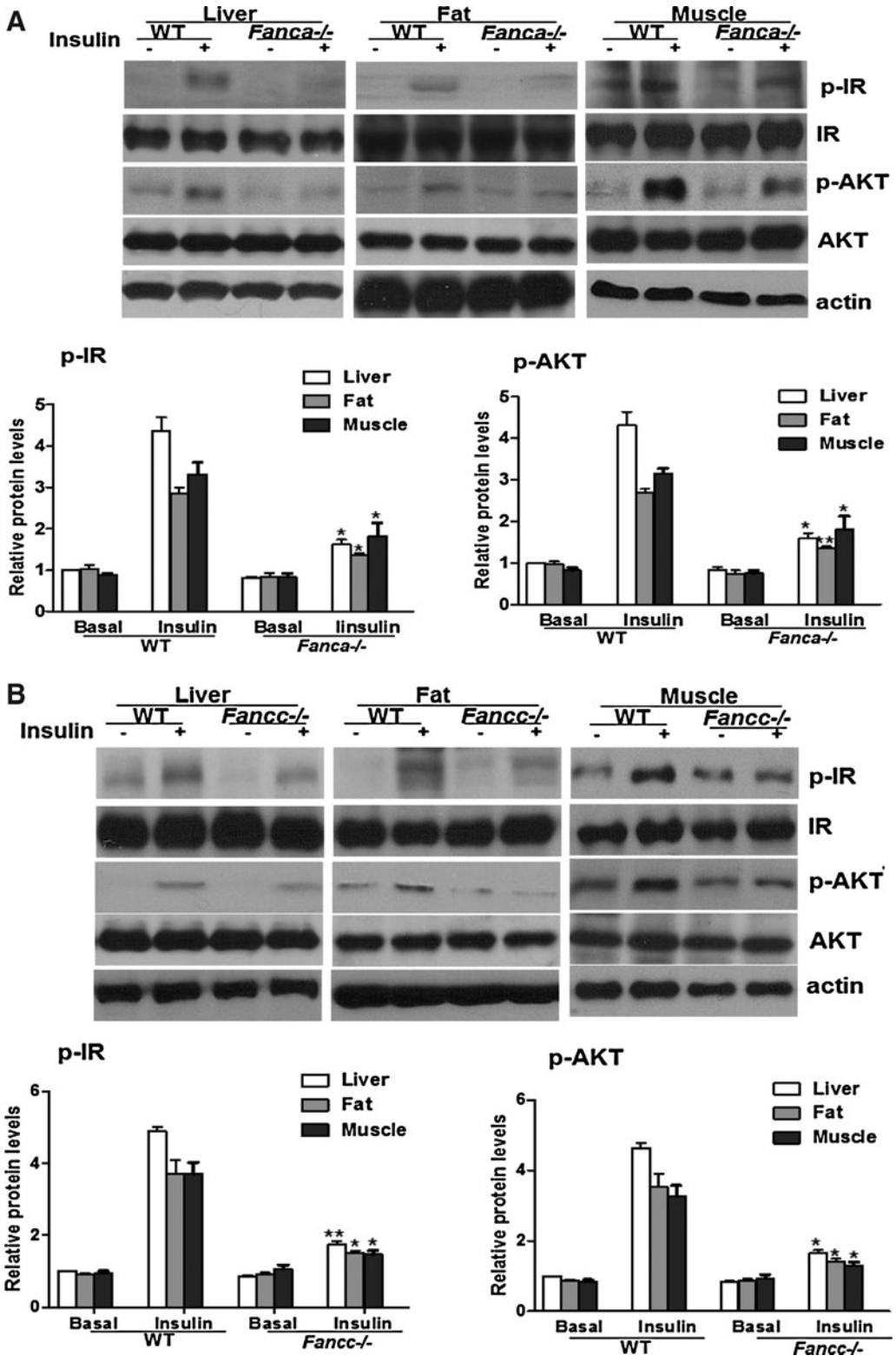

FIG. 4. Decreased IR$^{Tyr1158/1162/1163}$ phosphorylation in FA mice. (A, B) *Fanca*$^{-/-}$ **(A)** or *Fancc*$^{-/-}$ **(B)** and wt littermates were fasted overnight followed with an injection of saline or insulin (5 U/Kg of body weight), and tissue samples were collected 10 min after the injection. Western blot analysis of IR and AKT was performed by separating freshly prepared tissue homogenates on an SDS-PAGE gel and probed with antibodies against phosphorylated IR (p-IR) Tyr1158/1162/1163 and total IR (beta-subunit), or AKTSer308 (p-AKT) and total AKT. The data are presented as mean ± SD. *$p < 0.05$, **$p < 0.01$ for *Fanca*$^{-/-}$ or *Fancc*$^{-/-}$ mice *versus* WT mice. **(C)** HepG2 cells transduced with lentivirus carrying shRNA for the human *FANCA* or *FANCC* gene were starved overnight and treated with insulin (10 μg/ml) for 15 min. Cell lysates were separated with SDS-PAGE and probed with antibodies against p-IR, IR, p-AKT, AKT, FANCA, FANCC, and actin. Protein band intensities were analyzed using ImageJ software. The level of each phosphorylated form or its corresponding total protein was first normalized to that of actin and then, the ratio for the phosphorylated form/total protein was calculated. The data are presented as mean ± SD. *$p < 0.05$, **$p < 0.01$ versus the control groups.

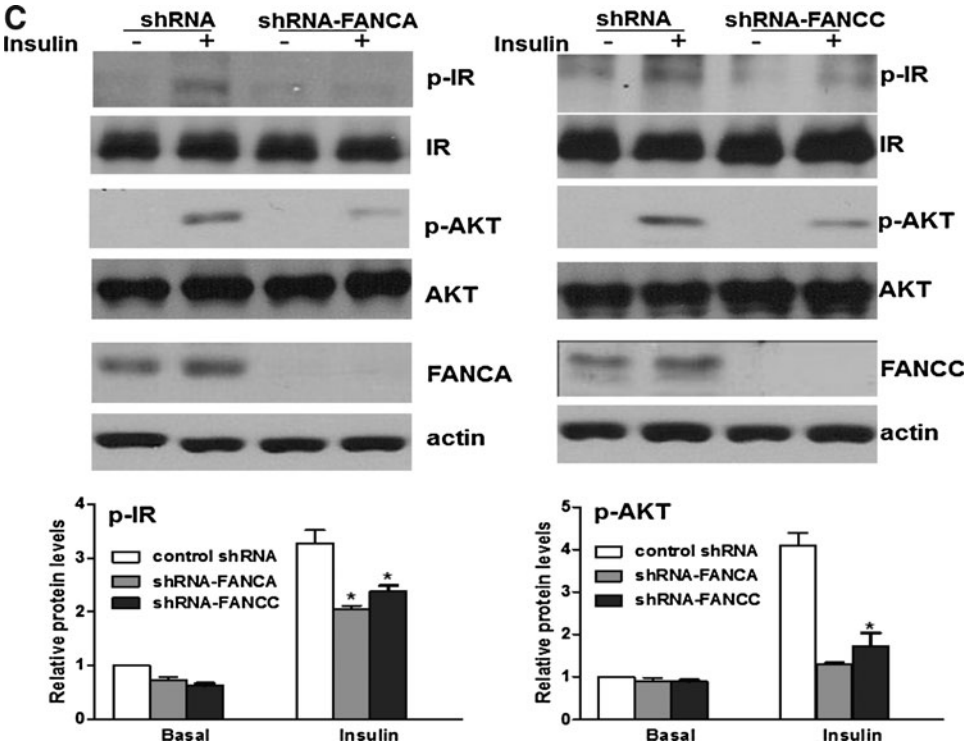

FIG. 4. (Continued).

ROS contribute to impaired insulin signaling in FA deficiency

Previous studies suggested that ROS could cause insulin resistance (16). In FA, one physiological source of ROS is the pro-inflammatory cytokine tumor necrosis factor alpha (TNF-α) (25, 34, 38). To establish the link between ROS and insulin resistance, we treated FA mice with TNF-α to produce physiologically relevant ROS. Flow cytometric analysis shows that TNF-α markedly increased ROS in beta cells isolated from *Fanca*$^{-/-}$ mice compared with the vehicle-treated animals (Fig. 5A), which could be completely eliminated by Quercetin (3,5,7,3′,4′-pentahydroxy-flavone), a natural ROS scavenger (Fig. 5A). It should be noted that a high-fat diet did not significantly increase ROS production in either WT or *Fanca*$^{-/-}$ mice compared with normal chow (Supplementary Fig. S7).

We next determined the contribution of ROS to FA insulin resistance *in vitro* and *in vivo*. First, we used the anti-oxidant Quercetin to analyze the effect of TNF-α-generated ROS on insulin signaling in beta cells isolated from WT and *Fanca*$^{-/-}$ mice. TNF-α treatment decreased the insulin-induced tyrosine phosphorylation of IR and IRS-1 but increased the serine phosphorylation of IRS-1 on residue 307 (Fig. 5B), which was reported to inhibit IR-stimulated IRS-1 tyrosine phosphorylation (1). Remarkably, Quercetin treatment completely reversed the inhibitory effect of TNF-α (Fig. 5B). Next, we investigated the *in vivo* effect of TNF-α-generated ROS on the insulin signaling. We pretreated WT or *Fanca*$^{-/-}$ mice with Quercetin followed by the TNF-α injection. The mice were then fasted and injected with insulin, and liver, fat, and muscle tissues were isolated and analyzed for ROS production and insulin signaling. We observed significantly increased ROS accumulation in all three insulin-responsive tissues from TNF-α-treated *Fanca*$^{-/-}$ mice compared with WT controls; whereas Quercetin pretreatment completely eliminated TNF-α-generated ROS in those tissues (Fig. 5C). Biochemical analysis shows that TNF-α treatment decreased the insulin-stimulated tyrosine phosphorylation of IR and IRS-1 in the tested tissues from mice of both genotypes (Fig. 5D). Interestingly, a more robust increase in the level of inhibitory IRS-1^{Ser307} was repeatedly found in TNF-α-treated *Fanca*$^{-/-}$ mice relative to WT controls (Fig. 5D). Again, Quercetin effectively restored insulin signaling in both genotypes, as demonstrated by the increased tyrosine phosphorylation of IR and IRS-1 and decreased inhibitory IRS-1^{Ser307} (Fig. 5D).

Quercetin ameliorates FA insulin resistance

We next investigated the role of TNF-α-generated ROS on FA diabetes-prone phenotypes *in vivo*. We treated *Fanca*$^{-/-}$ and WT mice with TNF-α to produce physiological oxidative stress. The mice were also treated for 10 days with daily injections of Quercetin or vehicle followed by four sets of analyses: fasting blood glucose, whole-body sensitivity to glucose or insulin in response to glucose or insulin challenge using the GTT or ITT, and HFD-induced weight gain. TNF-α significantly increased fasting-blood glucose in *Fanca*$^{-/-}$ mice compared with WT animals, whereas co-treatment with Quercetin largely prevented this increase (Fig. 6A). We observed no statistical difference in the levels of fasting blood glucose in WT mice treated with or without Quercetin (Fig. 6A). GTT test shows that Quercetin treatment significantly decreased whole-blood glucose in *Fanca*$^{-/-}$ mice 15 min after glucose challenge (Fig. 6B). Similarly, in response to insulin challenge, there was a significant decrease in the blood

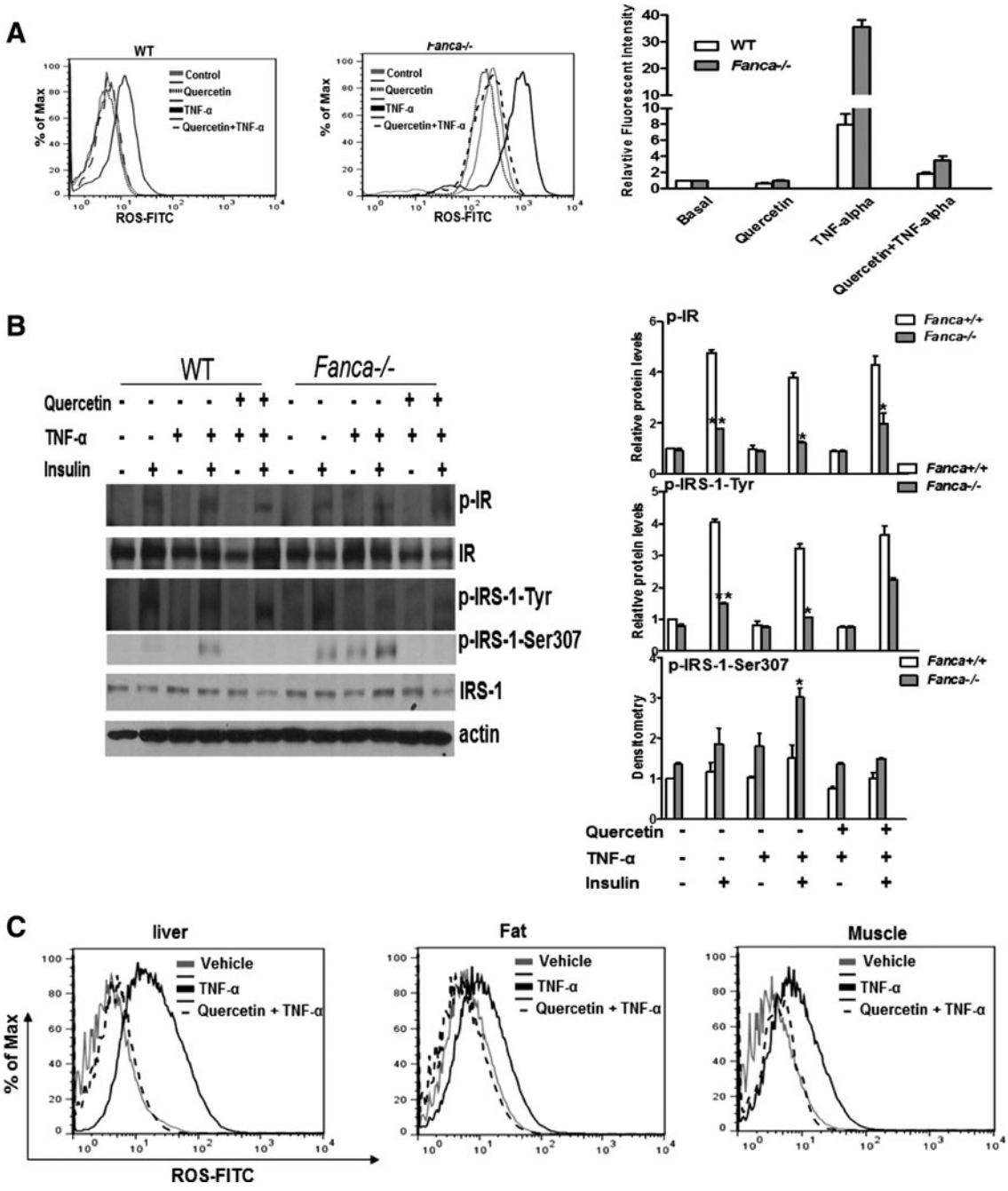

FIG. 5. TNF-α-generated ROS contribute to decreased-IR signaling. (A) Beta cells isolated from wt and *Fanca*$^{-/-}$ mice were treated with saline, TNF-α, Quercetin, or TNF-α and Quercetin. Cells were labeled with FITC-conjugated CM-H2DCFDA, and ROS production was examined by flow cytometry. **(B)** Beta cells were treated with or without TNF-α for 30 min, followed by insulin (10 μg/ml) for 15 min. Quercetin treatment was given 30 min before TNF-α treatment. Cell lysates were analyzed by immunoblotting. **(C)** The indicated mice (2–3 months old, $n = 6$–8 each group) were injected with Quercetin (50 mg/Kg) twice per week for 3 weeks, followed by a single TNF-α (100 μg/Kg) injection. Liver, fat, and muscle were collected, and a single-cell suspension was prepared. ROS production was examined by flow cytometry with H2DCFDA staining. **(D)** Mice were treated as described in **(C)**, fasted overnight after the final injection, and given an injection of insulin (5 U/Kg). After 10 min, the liver, fat, and muscle were collected, and the expression of insulin signaling components was analyzed by immunoprecipitation and western blotting. Protein band intensities were analyzed using ImageJ software. The level of each phosphorylated form or its corresponding total protein was first normalized to that of actin and then, the ratio for the phosphorylated form/total protein was calculated. The data are presented as mean ± SD. $^{*}p < 0.05$, $^{**}p < 0.01$ for *Fanca*$^{-/-}$ mice versus WT littermates. FITC, fluorescein isothiocyanate; ROS, reactive oxygen species; TNF-α, tumor necrosis factor alpha.

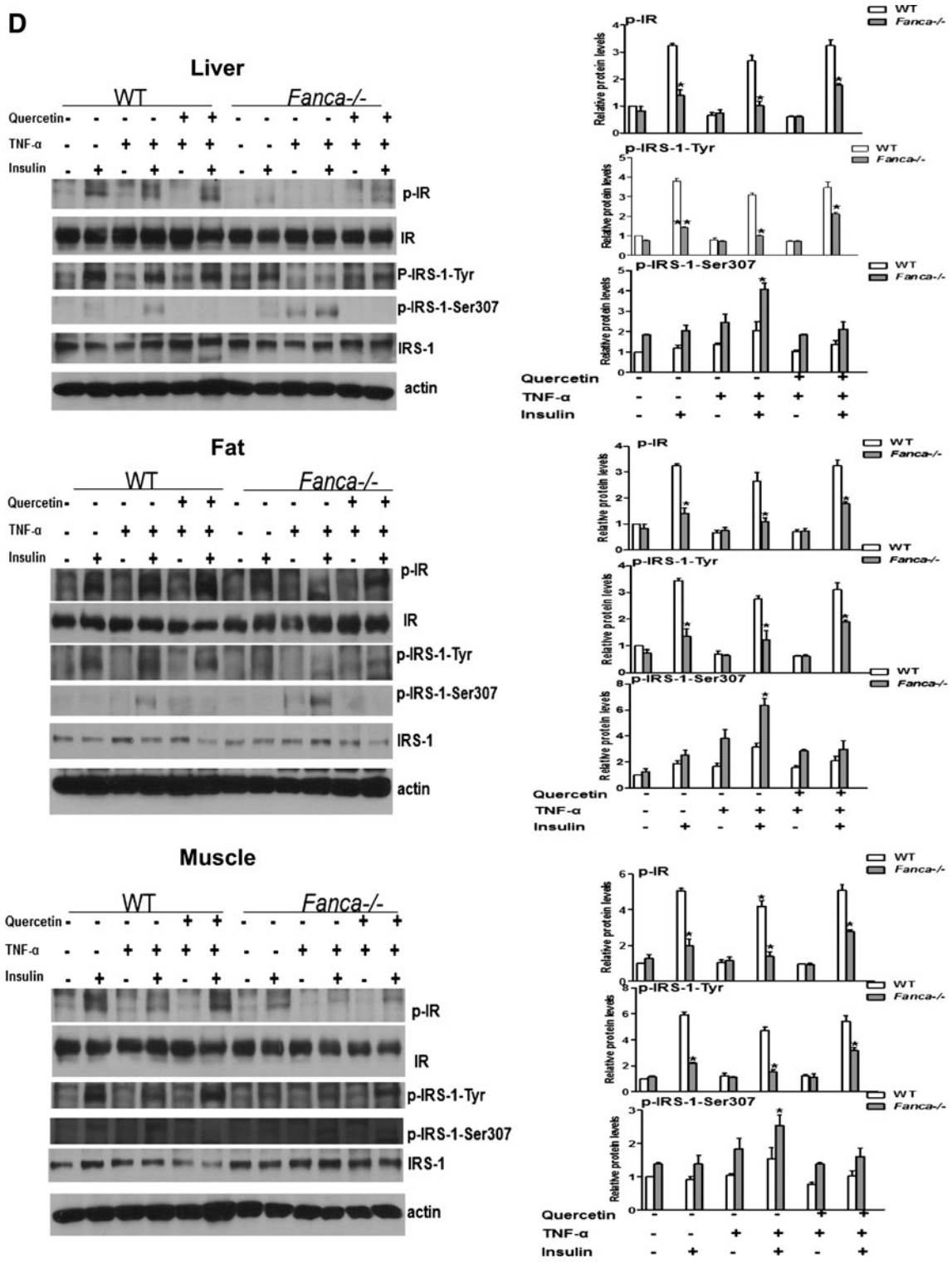

FIG. 5. (Continued).

glucose level at 45 min postinsulin injection in Quercetin-treated *Fanca*$^{-/-}$ mice compared with the vehicle-treated controls (Fig. 6C). Moreover, Quercetin partially reversed the HFD-induced obesity in *Fanca*$^{-/-}$ mice, with weight gain being not statistically different from that of normal diet-fed animals (Fig. 6D). Together, these results demonstrate that the anti-oxidant Quercetin can effectively prevent the FA hyperglycemic phenotypes as well as HFD-induced obesity in mice, confirming the causal role of ROS in FA insulin resistance.

Screen for factors that mediate ROS effect on insulin resistance

To gain insights into the molecular mechanism by which ROS induce insulin resistance, we sought to identify the

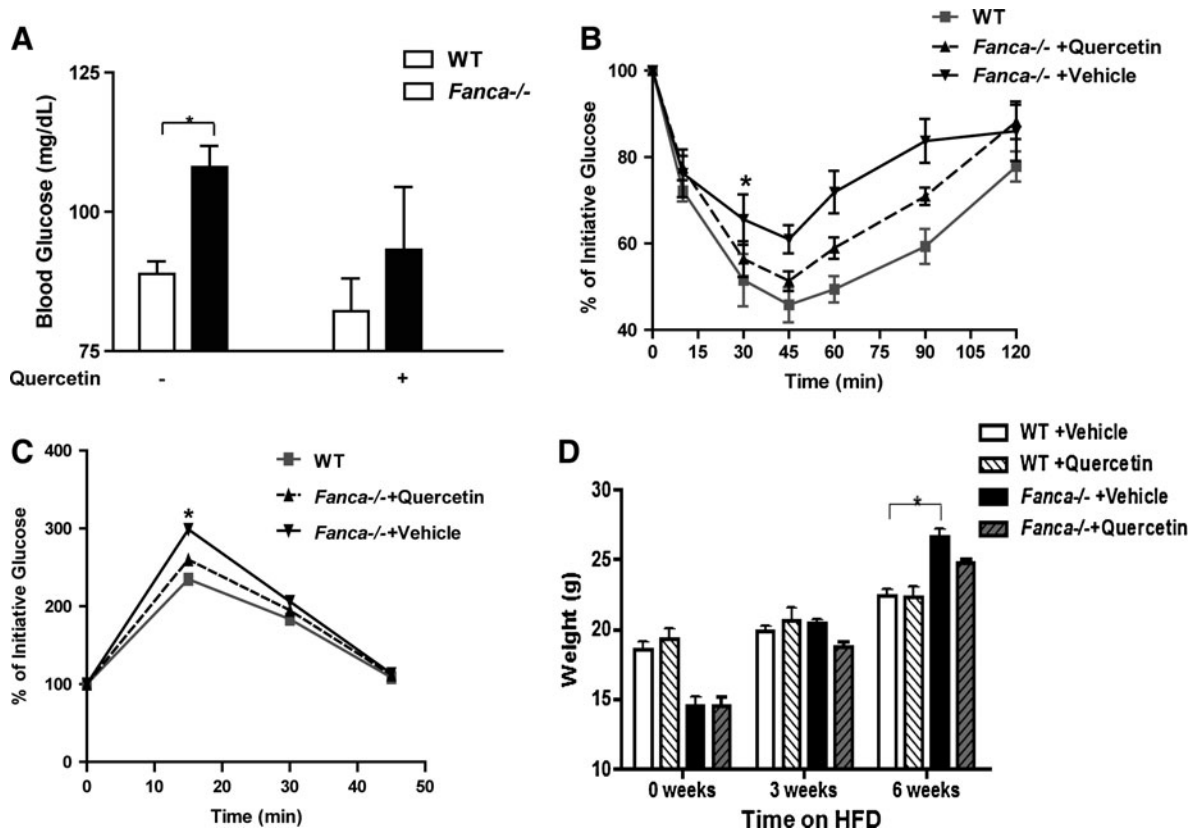

FIG. 6. Quercetin attenuates the diabetes phenotype in FA mice. (A) *Fanca*+/+ and *Fanca*$^{-/-}$ mice (3–4 months old, $n=6$–8 each group) were injected with Quercetin (50 mg/Kg) twice per week for 2 weeks. After the final injection, whole-blood glucose was measured in mice fasted overnight by using tail blood. The data are presented as mean ± SD. *$p<0.05$ for *Fanca*$^{-/-}$ mice versus *Fanca*+/+ mice. **(B, C)** The mice as described in **(A)** were fasted and given an injection (IP) of either glucose (1 g/Kg of body weight) **(B)** or insulin (1.0 U/Kg of body weight) **(C)**, and whole-blood glucose was examined at the indicated time points by using the glucometer. The results are shown as the percentage of the initial glucose levels. *$p<0.05$ for *Fanca*$^{-/-}$ mice versus *Fanca*+/+ mice, or *Fanca*$^{-/-}$ mice injected with Quercetin versus those with vehicle. **(D)** *Fanca*+/+ and *Fanca*$^{-/-}$ mice (6–7 weeks old, $n=6$–8 each group) were fed with HFD and injected with Quercetin (50 mg/Kg) twice per week for 6 weeks. The weight was examined at the indicated time points of the Quercetin treatment. The results are shown as the original readout. *$p<0.05$ for *Fanca*$^{-/-}$ fed with HFD without Quercetin treatment versus *Fanca*+/+ mice.

factors that mediated the inhibitory effect of ROS on insulin signaling. To this end, we screened for inhibitors that could rescue insulin signaling in FA cells. Since *in vitro* and *in vivo* results clearly demonstrated that ROS-induced FA insulin resistance results from reduced IR phosphorylation ($IR^{Tyr1158/1162/1163}$) and/or increased IRS-1 serine phosphorylation ($IRS\text{-}1^{Ser307}$), we focused on targeting these two molecular events by blocking the kinases with specific inhibitors or knocking down protein-kinases phosphatases by shRNA. It has been shown that protein-tyrosine phosphatases (PTPs) PTP-α, PTP-1B, and LAR can dephosphorylate and, thus, deactivate IR in a variety of experimental settings, although a consensus has not emerged as to whether any one or all of these PTPases play a physiological role in inactivating insulin signaling under physiological conditions (7, 24, 40). On the other hand, increased ROS accumulation is known to activate JNK, which phosphorylates IRS-1 on Ser307 and causes insulin resistance (15, 19). The PKR has also been shown to directly phosphorylate $IRS\text{-}1^{Ser307}$ and be deregulated in FA cells (35, 48, 50). The primary screen was performed to identify the kinases or phosphatases involved in insulin signaling. We subjected stably transduced HepG2 cells carrying the lentiviral shRNA targeting human *FANCA* gene either to each inhibitor or to PTPs knockdown. We then examined the effect of each compound or PTP knockdown on TNF-α-induced insulin resistance by analyzing the level of $IR^{Tyr1158/1162/1163}$ and $IRS\text{-}1^{Ser307}$. We anticipated that the amelioration of TNF-α-induced insulin resistance could be achieved only by compound(s) that would both restore IR tyrosine phosphorylation and suppress inhibitory $IRS\text{-}1^{Ser307}$ phosphorylation. The initial set of screens shows that PKR inhibitor II suppressed IRS-1Ser307 phosphorylation (Fig. 7A); whereas a PTP-α shRNA was able to increase IR tyrosine phosphorylation (Fig 7B). The inhibitors for PTP-1B, PTP-1D, LAR, and JNK showed no effect on TNF-α-induced insulin resistance, as demonstrated by no change in the level of $IR^{Tyr1158/1162/1163}$ or $IRS\text{-}1^{Ser307}$ (Supplementary Fig. S8).

Since either of the two inhibitors identified from the primary screen could not rescue both steps of FA insulin resistance, that is, restore IR tyrosine phosphorylation and suppress inhibitory $IRS\text{-}1^{Ser307}$ phosphorylation, we next performed a pairwise screen to evaluate the insulin-stimulated activation of the downstream kinase AKT in stably transduced HepG2 cells with combinations of inhibitors. Using this insulin-responsive

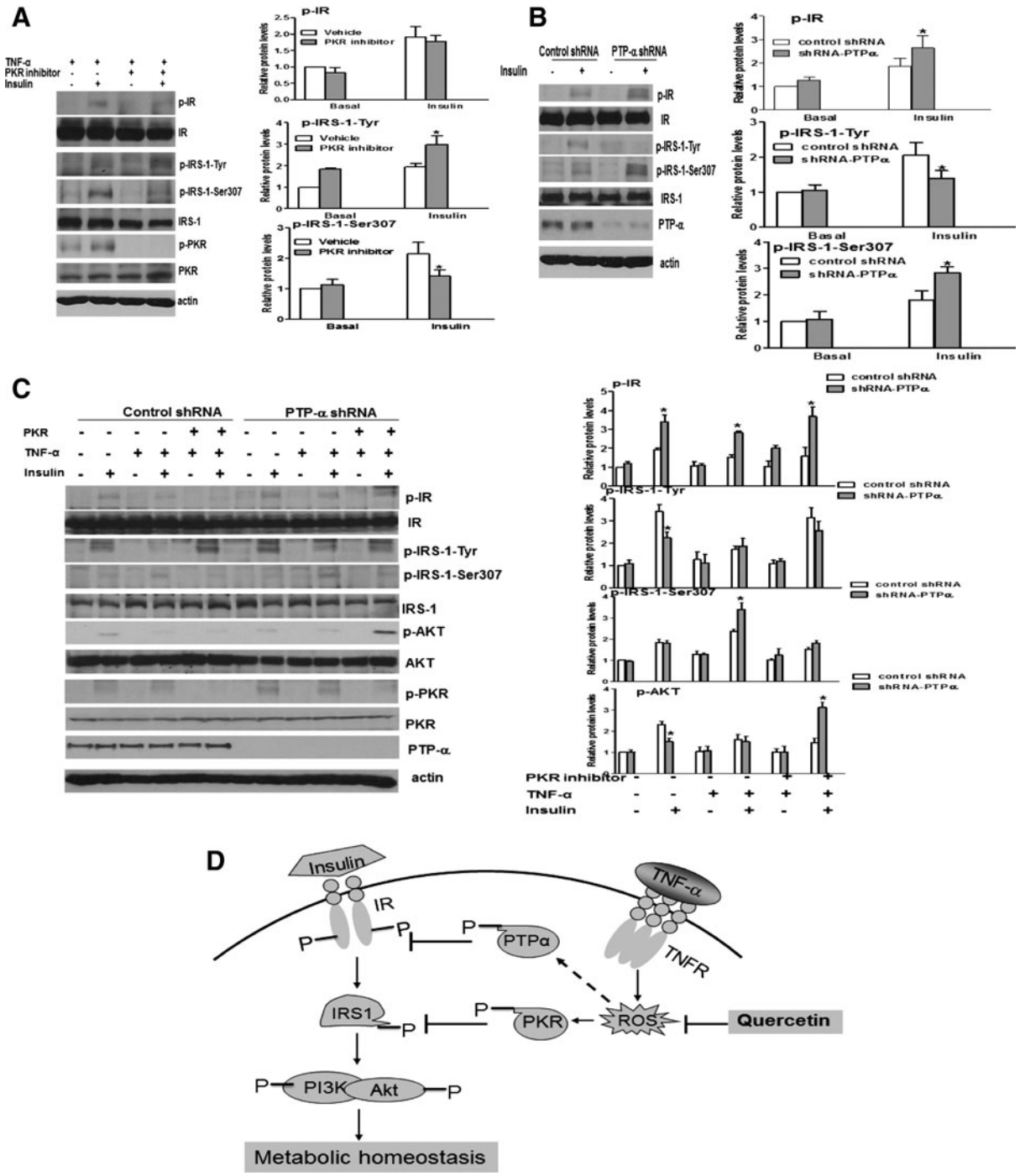

FIG. 7. Pair-wise screen identifies PTP-α and PKR inhibitors that rescue insulin resistance. (A) HepG2 cells transduced with a lentivirus carrying shRNA for the FANCA gene were pretreated with or without the PKR inhibitor (5 μM) for 30 min, followed by TNF-α at 10 μg/ml for 30 min, and insulin (10 μg/ml) for another 15 min. Cell lysates were analyzed with antibodies against p-IR, IR, p-IRS-1, IRS-1, PKR, or Actin. **(B)** The cells described in **(A)** were transduced with a lentivirus carrying shRNA for PTP-α and treated with or without insulin (10 μg/ml) for 15 min. Immunoprecipitation and immunoblotting were used to analyze p-IR and p-IRS-1 as well as PTP-α and Actin. **(C)** The cells described in **(B)** were pretreated with the PKR inhibitor II (5 μM) for 30 min, followed by TNF-α (10 μg/ml) for 30 min, and insulin (10 μg/ml) for another 15 min. Cell lysates were separated by SDS-PAGE and probed with antibodies against the indicated antibodies. Protein band intensities were analyzed using ImageJ software. The level of each phosphorylated form or its corresponding total protein was first normalized to that of actin and then, the ratio for the phosphorylated form/total protein was calculated. The data are presented as mean ± SD. $*p < 0.05$, $**p < 0.01$ versus the control groups. **(D)** A model for ROS-induced insulin resistance in FA. In this model, the overproduction of TNF-α results in the accumulation of ROS, a physiological phenomenon often found in FA patients. Elevated accumulation of ROS would affect two critical steps of IR signaling: (i) decrease IR tyrosine phosphorylation through PTP-α; (ii) increase inhibitory phosphorylation of IRS-1 by activation of PKR kinase, leading to insulin resistance and obesity. The natural anti-oxidant Quercetin proves effective in antagonizing the negative effect of ROS on insulin signaling and maintaining metabolic homeostasis. IRS, insulin receptor substrate; PKR, double-stranded RNA-dependent protein kinase; PTPs, protein-tyrosine phosphatases.

cell system, we were able to show that while PTP-α knockdown or the PKR inhibitor worked effectively in their respective target; either inhibitor by itself did not substantially alter the level of pAKT (Fig. 7). However, the combination of these two inhibitors completely normalized insulin-induced AKT activation in FANCA-deficient HepG2 cells (Fig. 7C). As expected, all other pairwise combinations failed to restore insulin signaling (Supplementary Fig. S9). Together, these results suggest that TNF-α-generated ROS target both PTP-α and PKR for FA insulin resistance.

Discussion

Insulin resistance, a state that precedes many clinical manifestations of the metabolic syndrome by inhibiting the action of insulin, is a key contributor to the pathogenesis of obesity and T2D mellitus (3, 13). Diabetes and other abnormalities of glucose metabolism are common among children and adolescents with FA, but the underlying molecular etiology of the diabetes remains to be elucidated (10, 11, 41). In this article, we show that mice deficient for the *Fanca* or *Fancc* gene seem to be diabetes- and obesity-prone. Mechanistically, we demonstrate that FA insulin resistance is associated with two critical molecular events in insulin signaling: a reduction in the tyrosine phosphorylation of IR and an increase in the inhibitory serine phosphorylation of IRS-1. Further, we show that high levels of ROS, accumulated spontaneously or generated by the pro-inflammatory cytokine TNF-α in several major insulin-sensitive tissues of FA mice, contribute to the FA insulin resistance. The treatment of FA mice with the natural anti-oxidant Quercetin restores IR signaling and ameliorates the diabetes- and obesity-prone phenotypes. The current study also identifies the factors that mediate the ROS effect on FA insulin resistance. Together, these findings establish a pathogenic and mechanistic link between ROS and insulin resistance in a unique human disease setting and highlight the fact that studying rare disorders can elucidate important new clinical and biological principles.

Oxidative stress, defined as an imbalance between the production of ROS and anti-oxidant defense, is associated with many disease states, including FA, which is arguably the only human genomic instability syndrome that is uniquely sensitive to oxidative stress (31). FA oxidant hypersensitivity has been documented in many studies using primary and immortalized cell cultures as well as *ex vivo* materials from patients (4, 20, 25, 31, 34). While FA murine models do not recapitulate some of the major FA clinical manifestations such as bone marrow failure and leukemia, cells from FA-deficient mice exhibit extreme oxidant sensitivity (25). All the observations indicated that the altered redox state in these FA mice was responsible for an impairment of cell proliferation or survival. In the context of metabolic disorders, it is also becoming increasingly apparent that oxidative stress accompanies insulin resistance, T2D, and obesity (3, 16, 18). The abnormal accumulation of ROS can contribute to insulin resistance by antagonizing insulin signaling, thereby impairing insulin-dependent glucose metabolism and contributing to insulin resistance (3, 16, 18). We have employed both cell-based and genetic models to establish a causal role of ROS in FA insulin resistance. First, the protein kinase array identified IR in response to oxidative stress is impaired in FA cells. Second, we demonstrate that TNF-α-induced FA insulin resistance is mediated by ROS. Third, Quercetin restores IR signaling and ameliorates the diabetes- and obesity-prone phenotypes as a consequence of ROS elimination. Finally, we have identified the molecular targets of ROS that are responsible for FA insulin resistance.

Our *in vivo* study shows that FA mice are highly susceptible to TNF-α-induced insulin resistance, and this is mediated by ROS. FA patients have abnormally high levels of TNF-α, which is a major mediator of inflammation and ROS production (25, 34, 38). It is conceivable that the presence of TNF-α and increased oxidative stress in FA may account for profound physiologic changes, including the development of insulin resistance and diabetes. TNF-α-induced inflammatory ROS can activate the stress kinase PKR (29, 35, 50). Indeed, our previous work shows that TNF-α induced persistent PKR activation in FA mice (35, 50). Increased ROS levels are known to stimulate PKR phosphorylation, a kinase linked to insulin resistance by interfering with IRS-1 activation (29). Specifically, PKR phosphorylates IRS-1 on Ser312 in human liver cells HepG2 (IRS-1^{Ser307} in mouse cells) (48). This inhibitory phosphorylation of IRS-1 blocks the tyrosine phosphorylation of IRS-1 by the IR. We envision that increased availability of TNF-α in FA would produce a high level of ROS, which, in turn, impairs insulin signaling through deregulation of the PKR activity. To test this notion, we performed inhibitor screens and identified PKR kinase as one of the two factors that mediate the ROS effect on FA insulin resistance.

The screen also identified the tyrosine phosphatase PTP-α as being the other factor that mediates ROS effect on FA insulin resistance. The regulation of IR tyrosine phosphorylation is a key step that is involved in the control of insulin signaling (6, 12). Augmented IR tyrosine dephosphorylation byPTPs may contribute to insulin resistance. PTP-α negatively regulates insulin signaling by dephosphorylating key tyrosine residues within the regulatory domain of the beta-subunit of IR and attenuates receptor tyrosine kinase activity. The inhibition of PTP-α is, therefore, anticipated to improve insulin resistance (24). The identification of PKR kinase and PTP-α phosphatase that mediate the inhibitory effect of ROS on insulin signaling provides a potential mechanistic link between ROS and insulin resistance. Strikingly, the inhibition of PKR failed to restore insulin signaling in FA cells (Fig. 7, Supplementary Fig. S5). Similarly, targeting PTP-α alone was not sufficient in rescuing FA insulin resistance. This suggests that the amelioration of FA insulin resistance may require simultaneously targeting both molecular events, which can both restore IR tyrosine phosphorylation and suppress inhibitory IRS-1^{Ser307} phosphorylation. Indeed, the combined inhibition of both PKR and PTP-α rescues FA insulin resistance caused by TNF-α in FANCA-knockdown cells (Fig. 7C).

The knockdown and rescue experiments using *FANCA* or *FANCC* shRNA and gene-corrected FA-A and FA-C, respectively, established a role of the FA proteins in insulin signaling (Fig. 4C, D, Supplementary Fig. S4). While the role of FA proteins in the prevention of insulin resistance remains to be elucidated, it is likely that FA proteins can function toward eliminating physiologic ROS in insulin-sensitive tissues. Indeed, we show that high levels of ROS are spontaneously accumulated in the liver, fat, and muscle tissues of FA mice (Supplementary Fig. 5C). To put this in perspective, we recently described an oxidative damage-specific interaction between FANCD2 and FOXO3a (26), a member of the

mammalian forkhead class O (FOXO) transcription factors that functions as a master regulator of oxidative stress (2, 32). Our study also shows that FANCD2-deficient cells exhibit a significant downregulation of the FOXO3a-targeting genes encoding superoxide dismutases (SOD1 and SOD2), glutathione peroxidase 1, and catalase involved in anti-oxidant defense (26). However, it is also possible that FA proteins themselves can directly influence the expression of antioxidant enzymes (such as glutathione S-transferases) or the biosynthesis of ROS metabolic molecules such as glutathione. Another possibility is that FA proteins can function toward disrupting downstream ROS signaling by protecting chromosomal DNA from ROS attack or facilitating the repair of oxidative DNA damage. FA patients are often found to have an overproduction of TNF-α (10, 25, 35, 38), and studies have shown that these physiologic ROS generated by TNF-α at inflammatory sites causes chromosomal DNA damage (9). It is perceivable that FA cells may be highly susceptible to an ROS attack or fail to repair oxidative DNA damage.

The current study used a number of anti-oxidants, including N-acetyl-L-cysteine and Quercetin, to detect the effect in the insulin resistance and diabetes. Among them, Quercetin was found to be less toxic in mice. Quercetin, a naturally occurring flavonoid found in a variety of fruits and green vegetables, has a wide range of biological activities such as free radical scavenging, iron chelating, ant-inflammation, and anti-cancer (21, 39). The ameliorative effect of Quercetin on FA insulin resistance induced by oxidative stress is mediated through decreasing ROS accumulation. This suggests that ROS generation is a necessary upstream event for FA insulin resistance. New insights on the potential role of oxidative stress in insulin resistance and on the action of natural antioxidants such as Quercetin may be therapeutically beneficial for patients with diabetes and obesity. Figure 7D illustrates a model, in which excessive ROS generated by the overproduction of TNF-α at inflammatory sites in disease state like FA, inhibit insulin signaling through two critical steps: decreasing IR phosphorylation by PTP-α phosphatase and increasing IRS-1 inhibitory phosphorylation by the PKR. Whether ROS acts directly on these enzymes or other unknown factors remains to be defined. The natural anti-oxidant Quercetin proves effective in antagonizing the negative effect of ROS on insulin signaling and maintaining metabolic homeostasis, and may be useful for therapies against insulin resistance-associated metabolic syndrome, as demonstrated in the FA disease model.

Materials and Methods

Chemicals and antibodies

All chemicals were purchased from Sigma unless indicated otherwise. Insulin for the mice injection was bought from the Novolin. Antibody against phosphor-IR (beta-subunit); phosphotyrosine (4G10) and p-PKR were from Millipore. The antibodies against phosphor-AKT (Thr 308, Ser 473), AKT, phosphor-JNK (Ser1186), JNK, PKR, PTP-1B and PTP1D, phosphor-IRS-1 (Ser 302, Ser 307), and IRS-1 were from Cell signaling Technology. The antibodies against Topo1 and beta-actin were from Santa Cruz Biotechnology and Sigma, respectively. The antibody against PTPalpha was purchased from Abcam, and the antibody against LAR was from BD Transduction Laboratories. 3T3-L1 preadipocyte and differentiation medium were purchased from Zen-Bio.

Mouse models

Fanca$^{-/-}$ and *Fancc*$^{-/-}$ mice were originally developed by and bred on the same genetic background (C57BL/6). All experimental mice used in this study were bred in our mouse facility and were 6–8 week-old at the start of the experiments. The mice were fed a Se-adequate diet, given free access to feed and distilled water, and housed in a constant temperature (22°C) animal room with a 12-h light/dark cycle. All experiments were approved by the Veterinary Services at Cincinnati Children's Hospital Medical Center and conducted in accordance with the National Institutes of Health guidelines for animal care.

HFD-fed mice

The mice were divided into two groups and either fed a HFD (Harlan Teklad) or received continuous feeding of a normal diet for approximately 3 months. On a caloric basis, the HFD consisted of 42% fat from lard, 42.7% carbohydrate, and 15.2% protein (total 4.5 Kcal/g), whereas the normal diet contained 11.4% fat, 62.8% carbohydrate, and 25.8% protein (total 3.0 Kcal/g). Food intake and body weight were measured once a week, and blood samples were taken at indicated time points from the intraorbital retrobulbar plexus from nonfasted anesthetized mice.

Cell culture

Human normal (JY) lymphoblastic cells, *FANCA*-deficient (HSC72) lymphoblastic cells, and *FANCC*-deficient (HSC536) lymphoblastic cells were incubated in RPMI 1640 containing 10% fetal bovine serum (FBS). Human liver hepatocellular cells HepG2 cells were cultured in DMEM containing 10% FBS. Mouse 3T3-L1 preadipocytes were from Dr. Mattew Grogg (CCHMC). 3T3-L1 cells were differentiated 1 day after 100% confluent (designated as day 0) by replacing the differentiation medium from Zen-Bio. After 3 days, the cells were maintained for an additional 2–4 days in the same medium, and fresh medium was replenished every other day. The cells were harvested after 7–10 days. Mouse beta-cell line NIT-1 was cultured in F-12K modified medium containing 10% Tet-approved FBS.

Knockdown by lentivirus

pLKO.1 lentiviral vector targeting human *FANCA* or *FANCC* was provided by Dr. Susanne Wells (CCHMC, OH). Hairpin sequence targeting *FANCA*, or *FANCC* were (GCCGACCTCAAGGTTTCTATA), or (CACGAGATCATT GGCTTTCTT), respectively. Hairpin sequence targeting the mouse *Fanca* (CGGGTTTATATCGAACGCAAT), *Fancc* (CGGGTTTATATCGAACGCAAT) or luciferase (CTTACGC TGAGTACTTCGA) was cloned into the pTRIPZ empty vector (Open Biosystems). The pLKO.1-TRC-cloning control was purchased from Addgene, and the hairpin sequence targeting human *PTPα*, *PTP1B*, *PTP1D* or *LAR* were (GCTGGACC TATGGGAATATTC), (GAAGCCCAAAGGAGTTACATT), (CGCTAAGAGAACTTAAACTTT), or (CCGAGGACTAT GAAACCACTA), respectively. The pLKO.1 lentiviruses expressing shRNA for *FANCA*, *FANCC*, *PTPα*, *PTP1B*, *PTP1D*, or *LAR* were used to transduce HepG2 cells; while the pTRIPZ

lentiviruses carrying shRNA for the mouse *Fanca* or *Fancc* gene were used to transduce the mouse beta-cell line NIT-1 or mouse adipocyte cell line 3T3-L1. Lentiviruses were prepared by the Vector Core of Cincinnati Children's Research Foundation (Cincinnati Children's Hospital Medical Center, Cincinnati, OH). Viral supernatant was collected at 36, 48, and 72 h, respectively, after transfection. For transduction, the cells were seeded at 6-cm plates overnight till ~70% confluent. At the 2nd day, virus particles were added to the cells and incubated overnight in the medium containing 4 μg/ml polybrene overnight followed by changing the fresh medium and continuing incubation for 48 h. After transduction, the cells were selected with 1 μg/ml puromycin (Sigma) or sorted by flow cytometry using Venus as a marker. For pTRIPZ shRNA vectors, transduced cells were selected for puromycin resistance, and induced with doxycycline (Clontech Laboratories, Inc.) for 72 h before experimentation.

Insulin measurement

Mice were IP injected with glucose (1 g/kg body weight), and whole blood was collected from tail vein samples at the indicated times. Insulin levels were measured in plasma by ELISA by using mouse insulin as a standard (Crystal Chem).

Body weight and food intake measurement

Food consumption and water intake index of every cage containing three to four mice were daily measured. Cumulative food intake (g/week) and water intake (ml/week) were calculated as follows: Cumulative food intake = total food consumption per week/body weight; water intake = total water intake per week/body weight.

Receptor tyrosine kinase array

Cell lysates were exacted with NP40 buffer (1% NP-40, 20 m*M* Tris-HCl (pH 8.0), 137 m*M* NaCl, 10% glycerol, 2 m*M* EDTA, 1 m*M* sodium orthovanadate, 2 m*M* sodium fluoride, 10 μg/ml Aprotinin, 10 μg/ml Leupeptin, and 10 μg/ml Pepstatin), and equal amounts of proteins were used to perform receptor tyrosine kinase arrays (RayBiotech) or (R&D Systems) according to the manufacturer's manuals. Phosphorylation status was determined by chemiluminescence and analyzed using the image analysis software Multi Gauge V3.0 (FUJIFILM) compared with the positive and negative controls.

Blood glucose

Mice ($n = 4$–6 per genotype) were fasted overnight for 8 h before determinations of whole-blood glucose at indicated time points. Whole-blood glucose was determined by clipping tails and using the Glucometer Elite system (Bayer) with Ascensia Elite blood glucose test strips as described by the manufacturer.

Insulin/glucose tolerance

WT and FA mice ($n = 8$–12 per genotype) that were 6 months old were fasted 8 h and then given an IP injection of either insulin (0.25 U/Kg) or glucose (1 g/Kg). Whole-blood glucose was determined at the indicated time points after the injection, and the data were presented as the original readout and the relative percentage of the initial levels.

Isolation of islets

Islets were obtained from 6- to 8-week-old male mice as previously described (5). Briefly, the mice were anesthetized, and pancreases were distended through the pancreatic duct with 2.5 ml of Hanks' balanced salt solution (Life Technologies) containing 2.0 mg/ml of collagenase (Type V; Sigma Chemical Co.). The distended pancreases were then removed and incubated at 37°C for 15 min. The islets were purified by discontinuous centrifugation on Ficoll (Sigma) gradients. After centrifugation, the islets were handpicked and cultured in HAM's F10 medium (Sigma) supplemented with 12 m*M* HEPES, 2 m*M* L-glutamine, 10% heat-inactivated fetal calf serum, 100 U/ml penicillin, and 100 μg/ml streptomycin in 95% air, 5% CO2 at 37°C.

Biochemical analysis of insulin signaling

For determination of insulin signaling in the liver, fat, and muscle tissues, the mice (6-months old, $n = 8$ per genotype) were fasted overnight (8 h) and were injected (IP) with insulin (5 U/kg). The mice were killed 10 min after the injection, and the tissues were excised and frozen in liquid nitrogen till further processing. The liver, fat, and muscle samples used for Western blot analysis were homogenized in buffer A (100 m*M* Tris, pH 7.4, 250 m*M* sucrose and protease inhibitor mixture [1 m*M* sodium pyrophosphate, 1 m*M* sodium orthovanadate, 10 μg/ml Leupeptin, 10 μg/ml Aprotinin, 1 μ*M* microcystin, 1 m*M* PMSF, and 10 m*M* sodium fluoride]). The samples used for immunoprecipitation were homogenized in buffer B (50 m*M* Hepes, pH 7.6, 100 m*M* sodium chloride, 1% Triton X-100, 5 m*M* EDTA, and protease inhibitor mixture as in buffer A). The tissue homogenates were centrifuged at 14,000 *g* for 10 min at 4°C, and protein concentration was determined by the Bio-Rad Protein Assay kit. The same amount of protein (100 μg) was separated by sodium dodecyl sulfate polyacrylamide gel electrophoresis (SDS-PAGE) following the immunoblotting analysis with the antibodies just described. For immunoprecipitation, the same amount of protein (500–1000 μg) was incubated with the antibody against IRS-1 and 50 μl of protein A/G-Sepharose beads overnight at 4°C with rotation. Then, the beads were washed four times with 1 ml buffer B at 4°C, and 5× SDS buffer (20 μl) was then added to the washed beads and used for Western blot analysis with the antibody against p-IRS-1^{Ser302} or p-IRS-1^{Ser307}. Protein band intensities were analyzed using ImageJ software. The level of each phosphorylated form or its corresponding total protein was first normalized to that of actin and then, the ratio for the phosphorylated form/total protein was calculated.

To determine insulin signaling in cultured cells, the cells were plated in the 100-mm tissue culture plate and starved overnight. After treatment as indicated, the reaction was stopped by ice-cold PBS containing sodium vanadate, and the cells were collected and lysed with NP-40 buffer (1% NP-40, 20 m*M* Tris-HCl (pH 8.0), 137 m*M* NaCl, 10% glycerol,2 m*M* EDTA, 1 m*M* sodium orthovanadate, 10 μg/mL Aprotinin, 10 μg/mL Leupeptin, and10 μg/mL Pepstatin). The related signaling proteins were examined as just described.

Statistical analysis

Data were analyzed by using the two-tailed, unpaired student's *t*-test or the one-Way analysis of variance using Prism 4.0 software (GraphPad Software, Inc.).

Acknowledgments

The authors thank Dr. Madeleine Carreau (Laval University, Canada) for the *Fanca*+/− mice; Dr. Yi Zheng and Dr. James M. Wells at the Cincinnati Children's Hospital Medical Center for their comments on this work. They also thank Dr. Susanne Wells (Cincinnati Children's Hospital Medical Center) for pLKO.1-Puro, pLKO.1-FANCA, and pLKO.1-FANCC lentiviral vectors; Dr. Bob Opoka (Cincinnati Children's Hospital Medical Center) for technical advice; and the Vector Core of the Cincinnati Children's Research Foundation (Cincinnati Children's Hospital Medical Center) for the preparation of retrovirus and lentiviruses.

This work was supported in part by the National Institutes of Health (grants R01 CA109641 and R01 HL076712). Q.P. is supported by a Leukemia and Lymphoma Scholar award.

Author Disclosure Statement

The authors have nothing to disclose.

References

1. Aguirre V, Werner ED, Giraud J, Lee YH, Shoelson SE, and White MF. Phosphorylation of Ser307 in insulin receptor substrate-1 blocks interactions with the insulin receptor and inhibits insulin action. *J Biol Chem* 277: 1531–1537, 2002.
2. Ambrogini E, Almeida M, Martin-Millan M, Paik JH, Depinho RA, Han L, Goellner J, Weinstein RS, Jilka RL, O'Brien CA, and Manolagas SC. FoxO-mediated defense against oxidative stress in osteoblasts is indispensable for skeletal homeostasis in mice. *Cell Metab* 11: 136–146, 2010.
3. Andrikopoulos S, Blair AR, Deluca N, Fam BC, and Proietto J. Evaluating the glucose tolerance test in mice. *Am J Physiol Endocrinol Metab* 295: E1323–E1332, 2008.
4. Bagby GC, Jr. Genetic basis of Fanconi anemia. *Curr Opin Hematol* 10: 68–76, 2003.
5. Carter JD, Dula SB, Corbin KL, Wu R, and Nunemaker CS. A practical guide to rodent islet isolation and assessment. *Biol Proced Online* 11: 3–31, 2009.
6. Chakraborty A, Koldobskiy MA, Bello NT, Maxwell M, Potter JJ, Juluri KR, Maag D, Kim S, Huang AS, Dailey MJ, Saleh M, Snowman AM, Moran TH, Mezey E, and Snyder SH. Inositol pyrophosphates inhibit Akt signaling, thereby regulating insulin sensitivity and weight gain. *Cell* 143: 897–910, 2010.
7. Cheung AT, Wang J, Ree D, Kolls JK, and Bryer-Ash M. Tumor necrosis factor-alpha induces hepatic insulin resistance in obese Zucker (fa/fa) rats via interaction of leukocyte antigen-related tyrosine phosphatase with focal adhesion kinase. *Diabetes* 49: 810–819, 2000.
8. Cumming RC, Lightfoot J, Beard K, Youssoufian H, O'Brien PJ, and Buchwald M. Fanconi anemia group C protein prevents apoptosis in hematopoietic cells through redox regulation of GSTP1. *Nat Med* 7: 814–820, 2001.
9. Dufour C, Corcione A, Svahn J, Haupt R, Poggi V, Béka'ssy AN, Scimè R, Pistorio A, and Pistoia V. TNF-alpha and IFN-gamma are overexpressed in the bone marrow of Fanconi anemia patients and TNF-alpha suppresses erythropoiesis *in vitro*. *Blood* 102: 2053–2059, 2003.
10. Elder DA, D'Alessio DA, Eyal O, Mueller R, Smith FO, Kansra AR, and Rose SR. Abnormalities in glucose tolerance are common in children with fanconi anemia and associated with impaired insulin secretion. *Pediatr Blood Cancer* 51: 256–260, 2008.
11. Giri N, Batista DL, Alter BP, and Stratakis CA. Endocrine abnormalities in patients with Fanconi anemia. *J Clin Endocrinol Metab* 92: 2624–2631, 2007.
12. Gual P, Le Marchand-Brustel Y, and Tanti JF. Positive and negative regulation of insulin signaling through IRS-1 phosphorylation. *Biochimie* 87: 99–109, 2005.
13. Guilherme A, Virbasius JV, Puri V, and Czech MP. Adipocyte dysfunctions linking obesity to insulin resistance and type 2 diabetes. *Nat Rev Mol Cell Biol* 9: 367–377, 2008.
14. Hayes GR and Lockwood DH. Role of insulin receptor phosphorylation in the insulinomimetic effects of hydrogen peroxide. *Proc Natl Acad Sci U S A* 84: 8115–8119, 1987.
15. Hirosumi J, Tuncman G, Chang L, Görgün CZ, Uysal KT, Maeda K, Karin M, and Hotamisligil GS. A central role for JNK in obesity and insulin resistance. *Nature* 420: 333–336, 2002.
16. Houstis N, Rosen ED, and Lander ES. Reactive oxygen species have a causal role in multiple forms of insulin resistance. *Nature* 440: 944–948, 2006.
17. Jiang ZY, Zhou QL, Coleman KA, Chouinard M, Boese Q, and Czech MP. Insulin signaling through Akt/protein kinase B analyzed by small interfering RNA-mediated gene silencing. *Proc Natl Acad Sci U S A* 100: 7569–7574, 2003.
18. Kahn SE and Hull RL, Utzschneider KM. Mechanisms linking obesity to insulin resistance and type 2 diabetes. *Nature* 444: 840–846, 2006.
19. Kaneto H, Nakatani Y, Miyatsuka T, Kawamori D, Matsuoka TA, Matsuhisa M, Kajimoto Y, Ichijo H, Yamasaki Y, and Hori M. Possible novel therapy for diabetes with cell-permeable JNK-inhibitory peptide. *Nat Med* 10: 1128–1132, 2004.
20. Kennedy RD and D'Andrea AD. The Fanconi Anemia/BRCA pathway: new faces in the crowd. *Genes Dev* 19: 2925–2940, 2005.
21. Kobori M, Masumoto S, Akimoto Y, and Takahashi Y. Dietary quercetin alleviates diabetic symptoms and reduces streptozotocin-induced disturbance of hepatic gene expression in mice. *Mol Nutr Food Res* 53, 859–868, 2009.
22. Krüger M, Kratchmarova I, Blagoev B, Tseng YH, Kahn CR, and Mann M. Dissection of the insulin signaling pathway via quantitative phosphoproteomics. *Proc Natl Acad Sci U S A* 105: 2451–2456, 2008.
23. Kubota T, Kubota N, Kumagai H, Yamaguchi S, Kozono H, Takahashi T, Inoue M, Itoh S, Takamoto I, Sasako T, Kumagai K, Kawai T, Hashimoto S, Kobayashi T, Sato M, Tokuyama K, Nishimura S, Tsunoda M, Ide T, Murakami K, Yamazaki T, Ezaki O, Kawamura K, Masuda H, Moroi M, Sugi K, Oike Y, Shimokawa H, Yanagihara N, Tsutsui M, Terauchi Y, Tobe K, Nagai R, Kamata K, Inoue K, Kodama T, Ueki K, and Kadowaki T. Impaired insulin signaling in endothelial cells reduces insulin-induced glucose uptake by skeletal muscle. *Cell Metab* 13: 294–307, 2011.
24. Lammers R, Møller NP, and Ullrich A. The transmembrane protein tyrosine phosphatase alpha dephosphorylates the insulin receptor in intact cells. *FEBS Lett* 404: 37–40, 1997.
25. Li J, Sejas DP, Zhang X, Qiu Y, Nattamai KJ, Rani R, Rathbun KR, Geiger H, Williams DA, Bagby GC, and Pang Q. TNF-alpha induces leukemic clonal evolution *ex vivo* in Fanconi anemia group C murine stem cells. *J Clin Invest* 117: 3283–3295, 2007.
26. Li J, Du W, Maynard S, Andreassen PR, and Pang Q. Oxidative stress-specific interaction between FANCD2 and FOXO3a. *Blood* 115: 1545–1548, 2010.
27. MacKay C, Déclais AC, Lundin C, Agostinho A, Deans AJ, MacArtney TJ, Hofmann K, Gartner A, West SC, Helleday T,

Lilley DM, and Rouse J. Identification of KIAA1018/FAN1, a DNA repair nuclease recruited to DNA damage by monoubiquitinated FANCD2. *Cell* 142: 65–76, 2010.
28. Morrell D, Chase CL, Kupper LL, and Swift M. Diabetes mellitus in ataxia-telangiectasia, Fanconi anemia, xeroderma pigmentosum, common variable immune deficiency, and severe combined immune deficiency families. *Diabetes* 35: 143–147, 1986.
29. Nakamura T, Furuhashi M, Li P, Cao H, Tuncman G, Sonenberg N, Gorgun CZ, and Hotamisligil GS. Double-stranded RNA-dependent protein kinase links pathogen sensing with stress and metabolic homeostasis. *Cell* 140: 338–348, 2010.
30. Nakashima I, Kato M, Akhand AA, Suzuki H, Takeda K, Hossain K, and Kawamoto Y. Redox-linked signal transduction pathways for protein tyrosine kinase activation. *Antioxid Redox Signal* 4: 517–531, 2002.
31. Negrini S, Gorgoulis VG, and Halazonetis TD. Genomic instability—an evolving hallmark of cancer. *Nat Rev Mol Cell Biol* 11: 220–228, 2010.
32. Ni YG, Wang N, Cao DJ, Sachan N, Morris DJ, Gerard RD, Kuro-O M, Rothermel BA, and Hill JA. FoxO transcription factors activate Akt and attenuate insulin signaling in heart by inhibiting protein phosphatases. *Proc Natl Acad Sci U S A* 104: 20517–20522, 2007.
33. Pagano G, Degan P, d'Ischia M, Kelly FJ, Nobili B, Pallardó FV, Youssoufian H, and Zatterale A. Oxidative stress as a multiple effector in Fanconi anaemia clinical phenotype. *Eur J Haematol* 75: 93–100, 2005.
34. Pang Q and Andreassen PR. Fanconi anemia proteins and endogenous stresses. *Mutat Res* 668: 42–53, 2009.
35. Pang Q, Keeble W, Diaz J, Christianson TA, Fagerlie S, Rathbun K, Faulkner GR, O'Dwyer M, and Bagby GC, Jr. Role of double-stranded RNA-dependent protein kinase in mediating hypersensitivity of Fanconi anemia complementation group C cells to interferon gamma, tumor necrosis factor-alpha, and double-stranded RNA. *Blood* 97: 1644–1652, 2001.
36. Park SJ, Ciccone SL, Beck BD, Hwang B, Freie B, Clapp DW, and Lee SH. Oxidative stress/damage induces multimerization and interaction of Fanconi anemia proteins. *J Biol Chem* 279: 30053–30059, 2004.
37. Rani R, Li J, and Pang Q. Differential p53 engagement in response to oxidative and oncogenic stresses in Fanconi anemia mice. *Cancer Res* 68: 9693–9702, 2008.
38. Rosselli F, Sanceau J, Gluckman E, Wietzerbin J, and Moustacchi E. Abnormal lymphokine production: a novel feature of the genetic disease Fanconi anemia. II. *In vitro* and *in vivo* spontaneous overproduction of tumor necrosis factor alpha. *Blood* 83: 1216–1225, 1994.
39. Skaper SD, Fabris M, Ferrari V, Dalle Carbonare M, and Leon A. Quercetin protects cutaneous tissue-associated cell types including sensory neurons from oxidative stress induced by glutathione depletion: cooperative effects of ascorbic acid. *Free Radic Biol Med* 22: 669–678, 1997.
40. Stoker AW. Protein tyrosine phosphatases and signalling. *J Endocrinol* 185: 19–33, 2005.
41. Swift M, Sholman L, and Gilmour D. Diabetes mellitus and the gene for Fanconi's anemia. *Science* 178: 308–310, 1972.
42. Taniguchi CM, Emanuelli B, and Kahn CR. Critical nodes in signalling pathways: insights into insulin action. *Nat Rev Mol Cell Biol* 7: 85–96, 2006.
43. Um SH, D'Alessio D, and Thomas G. Nutrient overload, insulin resistance, and ribosomal protein S6 kinase 1, S6K1. *Cell Metab* 3: 393–402, 2006.
44. Vepa S, Scribner WM, Parinandi NL, English D, Garcia JG, and Natarajan V. Hydrogen peroxide stimulates tyrosine phosphorylation of focal adhesion kinase in vascular endothelial cells. *Am J Physiol* 277: L150–158, 1999.
45. Verweij CL and Gringhuis SI. Oxidants and tyrosine phosphorylation: role of acute and chronic oxidative stress in T-and B-lymphocyte signaling. *Antioxid Redox Signal* 4: 543–551, 2002
46. Virkamäki A, Ueki K, and Kahn CR. Protein-protein interaction in insulin signaling and the molecular mechanisms of insulin resistance. *J Clin Invest* 103: 931–943, 1999.
47. Yamamura H. Redox control of protein tyrosine phosphorylation. *Antioxid Redox Signal* 4: 479–480, 2002.
48. Y Yang X, Nath A, Opperman MJ, and Chan C. The double-stranded RNA-dependent protein kinase differentially regulates insulin receptor substrates 1 and 2 in HepG2 cells. *Mol Biol Cell* 21: 3449–3458, 2010.
49. Youngren JF. Regulation of insulin receptor function. *Cell Mol Life Sci* 64: 873–891, 2007.
50. Zhang X, Li J, Sejas DP, Rathbun KR, Bagby GC, and Pang Q. The Fanconi anemia proteins functionally interact with the protein kinase regulated by RNA (PKR). *J Biol Chem* 279: 43910–43919, 2004.

Address correspondence to:
Dr. Qishen Pang
Division of Experimental Hematology and Cancer Biology
Cincinnati Children's Hospital Medical Center
3333 Burnet Ave.
Cincinnati, OH 45229

E-mail: qishen.pang@cchmc.org

Date of first submission to ARS Central, November 27, 2011; date of final revised submission, April 6, 2012; date of acceptance, April 7, 2012.

Abbreviations Used

FA = Fanconi anemia
FANCA = Fanconi anemia complementation group A
FANCC = Fanconi anemia complementation group C
GTT = glucose tolerance test
HFD = high-fat diet
H_2O_2 = hydrogen peroxide
IP = intraperitoneal
IR = insulin receptor
IRS = insulin receptor substrate
ITT = insulin tolerance test
JNK = c-Jun NH2-terminal kinase
LCLs = lymphoblastic cell lines
OSR = oxidative stress response
PKR = double-stranded RNA-dependent protein kinase
PTKs = protein tyrosine kinases
PTPs = protein-tyrosine phosphatases
ROS = reactive oxygen species
RTK = receptor tyrosine kinase
SDS-PAGE = sodium dodecyl sulfate polyacrylamide gel electrophoresis
T2D = type 2 diabetes
TNF-α = tumor necrosis factor alpha
WT = wild-type